# Determination of the Electron Affinity of the Acetyloxyl Radical ($CH_3COO$) by Low-Temperature Anion Photoelectron Spectroscopy and ab Initio Calculations

**Xue-Bin Wang, Hin-Koon Woo, and Lai-Sheng Wang***

*Department of Physics, Washington State University, 2710 University Drive, Richland, Washington 99354, and Chemical Sciences Division, Pacific Northwest National Laboratory, MS K8-88, P.O. Box 999, Richland, Washington 99352*

**Babak Minofar and Pavel Jungwirth***

*Institute of Organic Chemistry and Biochemistry, Academy of Sciences of the Czech Republic, and Center for Complex Molecular Systems and Biomolecules, Flemingovo nám. 2, 16610 Prague 6, Czech Republic*

*Received: January 9, 2006; In Final Form: March 7, 2006*

The electronic structure and electron affinity of the acetyloxyl radical ($CH_3COO$) were investigated by low-temperature anion photoelectron spectroscopy and ab initio calculations. Photoelectron spectra of the acetate anion ($CH_3COO^-$) were obtained at two photon energies (355 and 266 nm) and under three different temperatures (300, 70, and 20 K) with use of a new low-temperature ion-trap photoelectron spectroscopy apparatus. In contrast to a featureless spectrum at 300 K, a well-resolved vibrational progression corresponding to the OCO bending mode was observed at low temperatures in the 355 nm spectrum, yielding an accurate electron affinity for the acetyloxyl radical as 3.250 ± 0.010 eV. This experimental result is supported by ab initio calculations, which also indicate three low-lying electronic states observed in the 266 nm spectrum. The calculations suggest a 19° decrease of the OCO angle upon detaching an electron from acetate, consistent with the vibrational progression observed experimentally.

## Introduction

The acetyloxyl free radical ($CH_3COO$) along with formyloxyl (HCOO) are prototypes of higher carboxyl radicals (RCOO), which are present in atmospheric aerosols and combustion flames.[1−3] The acetyloxyl radical is also believed to be a possible intermediate in the bimolecular reaction of $CH_3O + CO$, an important process in atmospheric and combustion chemistry.[4,5] In addition, the reactivity and decomposition of the $CH_3COO$ radical play important roles in organic synthesis because it is a common organic reaction intermediate.[6−8] Despite its importance and seeming simplicity, the $CH_3COO$ radical poses considerable challenges to both experimental and theoretical studies. Experimental study of the $CH_3COO$ radical has been difficult partly due to its short lifetime.[7,9] In particular, its electron affinity (EA) is still not known accurately. Theoretical study has been complicated by the presence of several closely lying states and symmetry-breaking issues.[10−15] The order of the low-lying states and their symmetries are still not well understood.

Negative ion photoelectron spectroscopy (PES) is a powerful experimental technique to study the electronic structures of neutrals, particularly for short-lived species or even transition states.[16] In principle, PES of acetate should yield a direct measurement of the EA of the $CH_3COO$ radical from the adiabatic detachment energy (ADE) of the ground-state transition. In fact, two PES experiments of acetate ($CH_3COO^-$) have been reported previously.[17,18] However, the reported spectra showed a featureless long tail near the threshold region, and hence only a upper limit of the EA was estimated.[17,18] This is presumably due to the following facts: (1) the first excited state of the neutral is only ∼0.1−0.2 eV above the ground state[11] so the transitions to the ground state and the first excited state are partially overlapped; (2) the O−C−O angle of the neutral is ∼20° smaller than that of the anion,[11,12] resulting in a long vibrational progression of the bending mode (∼580 $cm^{-1}$);[11] and (3) severe hot band transitions as a result of insufficient or no cooling of the parent $CH_3COO^-$ anion in the PES experiment. The electronic structure, predissociation dynamics, and EA of the simpler formyloxyl radical (HCOO) have also been studied with the gas-phase negative ion PES technique.[19,20] Although the PES spectra of $HCOO^-$ were complicated, a definitely vibrational progression was resolved, giving rise to an accurate EA of 3.498 ± 0.015 eV for the formyloxyl radical.[19]

Electron affinity is a fundamental thermodynamic property of a molecule.[21] There have been quite a few experimental estimates of the EA of $CH_3COO$ employing a variety of techniques including ion equilibrium (3.38 eV),[22] electron-impact ion appearance energy (3.30 ± 0.20 eV; 3.28 eV),[23,24] electron attachment methods (3.179 ± 0.052 eV),[25] and anion photodetachment (3.40 ± 0.30; 3.47 ± 0.01 eV).[17,18] Among all these techniques, anion PES directly measures electron binding energies of anions, and in principle is the most accurate method to determine the EA of the corresponding neutral radicals from the 0−0 transition of the anion PES spectrum. However, in many cases the 0−0 transitions were not resolved due to the existence of hot bands and limited spectral resolution or simply cannot be detected due to too large anion−neutral geometry changes such that the Franck−Condon factor of the 0−0 transition is negligiable.[26] Because of the lack of consistency, the EA of $CH_3COO$ was not included in a recent review

* Address correspondence to these authors. E-mail: ls.wang@pnl.gov and pavel.jungwirth@uochb.cas.cz

10.1021/jp060138p CCC: $33.50 
Published on Web 03/30/2006

article on atomic and molecular EAs,[21] and was listed in a range of 3.18−3.47 eV in the NIST database.[27]

Here we report vibrationally resolved PES spectra of acetate using a newly developed low-temperature PES facility, as well as ab initio calculations. The anions were pre-cooled to 70 and 20 K nominal temperatures before performing the PES experiment. A well-resolved vibrational progression corresponding to the OCO bending mode was observed in the low-temperature experiment, compared to the featureless long tail observed at room temperature. The EA of $CH_3COO$ was measured accurately from the 0−0 transition to be 3.250 ± 0.010 eV, in good agreement with the accompanying ab initio calculations.

## Experimental Details

The experiment was carried out with a newly developed instrument that couples an electrospray ionization source (ESI) to a magnetic bottle time-of-flight photoelectron spectrometer.[28,29] The ESI source and the magnetic-bottle photoelectron spectrometer are similar to that described previously.[30] A key feature of the new instrument is its cooling capability, accomplished by attaching the cold head of a close cycle helium refrigerator to the ion trap where ions are accumulated and cooled via collisional cooling with a cold background gas. Acetate anions were transferred to the gas phase by electrospray ionization from a solution of 1 mM $CH_3COONa$ salt desolved in a $H_2O/CH_3OH$ (1/3 ratio) mixed solvent. After passing through a RF-only octopole ion guide and a quadrupole mass filter (operated in the RF-only mode), all anions were turned 90° via a quadruple ion bender and entered into a three-dimensional Paul trap for ion accumulation and collisional cooling. The temperature of the ion trap can be controlled from 10 to 400 K. The collisional background gas used was 0.1 mTorr $N_2$ for experiments down to 70 K or 0.1 mTorr helium mixed with 20% $H_2$ for temperatures below 70 K. The cooled ions were pulsed out of the trap at a 10 Hz repetition rate to a time-of-flight mass spectrometer. The $CH_3COO^-$ anions were selected and decelerated before being intercepted by a detachment laser beam in the interaction zone of the magnetic-bottle electron analyzer. In the current experiment, two detachment photon energies were used: 355 (3.496 eV) and 266 nm (4.661 eV) from a Nd:YAG laser. The detachment laser was operated at 20 Hz with the ion beam off on alternate shots for background subtraction. The photoelectrons were collected with nearly 100% efficiency by the magnetic-bottle and analyzed in a 5.2-m long electron flight tube. The electron energy resolution of the apparatus is $\Delta E/E \sim 2\%$, i.e., 20 meV for 1 eV electrons. Photoelectron time-of-flight spectra were collected and then converted to kinetic energy spectra, calibrated by the known spectra of $I^-$ and $ClO_2^-$.[31] The electron binding energy spectra presented were obtained by subtracting the kinetic energy spectra from the detachment photon energies.

## Computational Details

The adiabatic detachment energy of acetate was evaluated at the MP2 (projected values of unrestricted calculations for the open shell neutral species) and CCSD(T) levels employing the aug-cc-pvdz and aug-cc-pvtz levels (the latter basis only at the MP2 level). We checked for the convergence of the detachment energies in terms of basis set expansion and inclusion of electronic correlation. ADE was evaluated as the difference between the total energies of the anionic acetate and the neutral acetyloxyl radical, both in their optimized geometries. The ADE was also corrected for the zero point energies (ZPE), evaluated at the respective minima of the anionic and neutral species at the MP2 level with either the aug-cc-pvdz or aug-cc-pvtz basis set. Energies of low-lying excited states of the neutral radical were estimated at the TD-B3LYP/aug-cc-pvdz level of theory. All calculations were performed with the Gaussian 03 program package.[32]

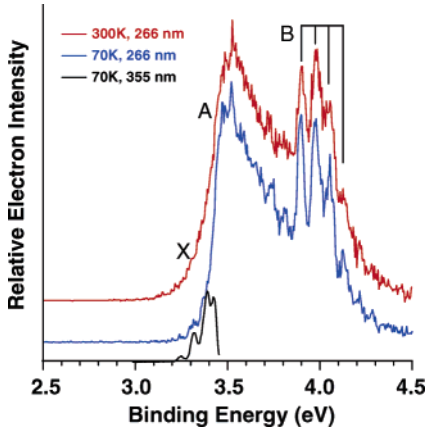


**Figure 1.** Photoelectron spectra of $CH_3COO^-$ at 266 nm (4.661 eV) and two ion-trap temperatures: 300 (red) and 70 K (blue). The 70 K spectrum at 355 nm (black) is also shown for comparison. The baselines of the three spectra are shifted relative to each other. The vertical lines represent the resolved vibrational structure.

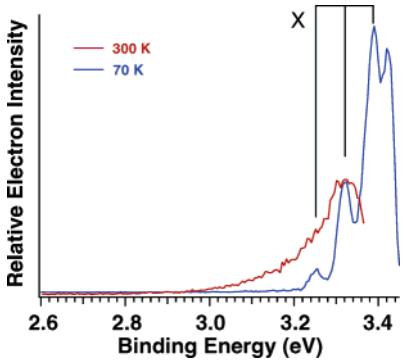


**Figure 2.** Photoelectron spectra of $CH_3COO^-$ at 355 nm (3.496 eV) and two ion-trap temperatures: 300 (red) and 70 K (blue). Note the early cutoff of the 300 K spectrum due to a small decelerating potential that exists sometimes, discriminating against very slow electrons. The vertical lines represent the resolved vibrational structure.

## Experimental Results

The photoelectron spectra of $CH_3COO^-$ were measured at two wavelengths (355 and 266 nm) under three different ion-trap temperatures: 300, 70, and 20 K, as shown in Figures 1 and 2. The 20 K spectra were almost identical with that at 70 K, but with lower count rates. Therefore only the 70 K and room temperature spectra are presented. Two broad bands were revealed at 266 nm, and only the threshold region was accessible at 355 nm.

Figure 1 shows the 266 nm spectra of $CH_3COO^-$ at both 300 (red) and 70 K (blue). The 355 nm spectrum at 70 K (black) is also displayed in Figure 1 for comparison. The two broad bands in the 266 nm spectra were partially overlapped. The first band was centered at 3.5 eV (A) with a long tail (X) extended to 3.1 eV, whereas the second band (B) was vibrationally resolved with a vibrational frequency of 620 ± 40 $cm^{-1}$. At 266 nm, the 70 K spectrum was only slightly improved, compared to the room-temperature data.

However, dramatically different spectra were observed at the two temperature regimes for the 355 nm spectra (Figure 2).

**TABLE 1: The Experimental Adiabatic Detachment Energy (ADE, in eV) of $CH_3COO^-$, Compared with ab Initio Calculations at Several Levels of Theory**

| | ADE[a] |
|---|---|
| experimental | $3.250 \pm 0.010$ |
| PMP2/aug-cc-pvdz | 3.24 |
| CCSD(T)/aug-cc-pvdz | 3.20 |
| PMP2/aug-cc-pvtz | 3.37 |
| CCSD(T)/aug-cc-pvtz (extrapolated) | 3.33 |

[a] The ADE is equivalent to the electron affinity of the neutral $CH_3COO$ radical.

While a featureless tail was observed at 300 K, the 70 K spectrum displayed a nicely resolved vibrational progression with a spacing of $545 \pm 40$ cm$^{-1}$ [the last peak at 3.42 eV was an artifact caused by the spectral cutoff at the 355 nm (3.496 eV) photon energy]. The 70 K spectrum at 355 nm was also shown in Figure 1. We note that the three vibrational peaks resolved at 355 nm line up with the discernible bumps in the cold 266 nm spectrum, which had poorer resolution and count rates in the threshold region. The early cutoff of the 300 K spectrum is due to a small decelerating potential that exists after a fresh baking of the detachment chamber, discriminating against very slow electrons, while the 70 K 355 nm spectrum was recorded at conditions with minimum deceleration effect (i.e., without baking for more than one week) to see a clear vibrational progression. All spectra were carefully calibrated, and except for the observable decelerating effect (cutoff at near photon energy range), spectra taken before and after a fresh baking are identical with the latter having a slightly better resolution. Figure 1 shows that the broad tail (X) in the room-temperature spectrum caused by hot band transitions makes it impossible to determine the detachment threshold with any reasonable accuracy. Assuming that the Franck−Condon factor for the 0−0 transition is not negligible (discussed in detail below), the first vibrational peak at 3.250 eV in the 70 K spectrum at 355 nm should represent the ADE of $CH_3COO^-$ and define the EA for the $CH_3COO$ neutral radical. As will be shown below, this experimental value is in good agreement with our ab initio calculations.

## Theoretical Results and Discussion

Upon electron detachment from the highest occupied molecular orbital, the resultant acetyloxyl radical undergoes a sizable geometry change in two parameters (all other bond lengths and bond angles remaining almost the same): at the MP2/aug-cc-pvdz level the C−C distance decreases from 1.56 to 1.49 Å and the O−C−O angle decreases from 129 to 110°. The adiabatic detachment energies corresponding to the lowest state of the neutral acetyloxyl radical are presented in Table 1. Note that the optimal geometry of the radical has two equivalent C−O bonds and its energy is practically insensitive to the rotation of the methyl group.[11] Values of the calculated ADE include the differential ZPE correction, which amounts (at the MP2/aug-cc-pvdz level) to +0.07 eV. Our best estimates for the ADE of the acetate anion, based on the independence of the MP2 → CCSD(T) and basis set extension effects at the CCSD(T) level, is 3.33 eV, with convergence being within 0.1 eV (Table 1). The present ADE can be compared to an older calculation by using the G2 scheme yielding a value of 3.36 eV.[12]

The fact that there are close lying occupied frontier orbitals in the acetate anion and the effect of symmetry breaking within the COO group, as well as the rotation of the methyl group, lead to a rather complex manifold of low-lying excited electronic states of the acetyloxyl radical.[11,12,33] For the sake of semiquantitative comparison with the PES data we simply estimated the vertical positions of the lowest excited states by a TD-B3LYP/aug-cc-pvdz calculation at the optimal geometry of the ground-state radical. The two lowest lying electronic excited states of the neutral acetyloxyl radical were estimated to be 0.17 and 0.70 eV above the ground state, respectively.

According to the theoretical data, the first broad band (X&A) observed in the 266 nm spectra was clearly due to two overlapping electronic transitions, the ground state and the first excited state of $CH_3COO$. The second and vibrationally resolved band (B) in Figure 1 was then due to detachment transition to the second excited state of $CH_3COO$. The 0−0 transition for the B band was at 3.90 eV, giving an excitation energy of 0.65 eV, in good agreement with the energetics from TD-B3LYP. The observed 620 cm$^{-1}$ spacing in the B band corresponds to the OCO bending mode in the second excited state of $CH_3COO$. The overall energetics and the PES spectra for $CH_3COO^-$ are similar to those of $HCOO^-$.[19] However, the EA of $CH_3COO$ (3.250 eV) is lower than that of HCOO (3.498 eV), suggesting that the H atom is much more electron withdrawing in $HCOO^-$ than the methyl group in acetate.

Figure 1 in ref 11 displayed schematically the top four valence molecular orbitals (MOs) for acetate. They are oxygen lone pairs on the $-CO_2^-$ group. The HOMO of acetate mainly consists of a $\sigma^*$ in-plane antibonding orbital. Thus it is expected that the OCO bond angle would be reduced upon removal of an electron from the HOMO. The HOMO also involves a slight antibonding interaction between the carboxylate and the methyl group, consistent with the shortening of the C−C distance. The HOMO-1 and HOMO-2 of acetate involve a $\sigma$ in-plane bonding combination and an out-of-plane antibonding $\pi^*$ orbital, respectively. Similar frontier MOs are obtained for the benzoate anions.[34] The 0.17 eV energy difference between the X and A states results in overlapping of the two electronic transitions and a broad feature in the PES spectrum, while a clearly OCO bending mode was observed in the B band.

One question concerning the 3.250 eV peak in the 355 nm spectrum at 70 K (Figure 2) was whether this peak truly represented the 0−0 transition. The limited spectral range and the complexity of the systems prevented us from performing a comprehensive Franck−Condon simulation. There were two other possibilities for this peak. One possibility was that it was due to a hot band transition. Then the second band at 3.32 eV would be the 0−0 transition. However, this assignment could be ruled out on the basis of two facts: (1) the spacing between the three vibrational peaks was fairly even and (2) under the low-temperature conditions the population of the vibrational hot band was expected to be negligible (<0.1%). The significant intensity of the 3.250 eV peak relative to the 3.32 eV peak suggested that it could not be due to a hot band in the OCO bending mode. The second possibility was that there was a negligible Franck−Condon factor (FCF) for the true 0−0 transition due to the large geometry change. In that case, the 3.250 eV peak would correspond to a transition to an excited vibrational level of the ground electronic state of $CH_3COO$ and could only define an upper limit for the ADE. However, this was also unlikely for two reasons. First, this assignment would indicate an EA smaller than 3.250 eV. Second, considering the relative shallowness of the bending potential, a 19° decrease of the OCO angle is unlikely to result in a negligible vibrational overlap between the ground state of $CH_3COO^-$ and that of $CH_3COO$. In fact, we estimated the ratio of the FCF for the 0 → 0 and 0 → 1 transitions considering only the OCO bending coordinate to be 1:4, consistent with the observed peak intensity.[35] Thus, considering both the experimental and theo-

retical results, we conclude that the 3.250 eV peak is the true 0−0 transition and does define the EA of the acetyloxyl radical with an uncertainty of ±0.010 eV. The calculated EA at various levels of theory (Table 1) is in good agreement with the experimental value.

**Acknowledgment.** The experimental work was supported by the U.S. Department of Energy (DOE), Office of Basic Energy Sciences, Chemical Science Division and was performed at the W. R. Wiley Environmental Molecular Sciences Laboratory, a national scientific user facility sponsored by DOE's Office of Biological and Environmental Research and located at Pacific Northwest National Laboratory, which is operated for DOE by Battelle. Supports from the Czech Ministry of Education (grants LC512 and ME644) and from the US-NSF (grants CHE-0431512 and CHE-0209719) for the theoretical work are gratefully acknowledged. We also thank Dr. Kai-Chung Lau at the Department of Chemistry, University of Chicago for estimating the Franck−Condon factors.

## References and Notes

(1) Atkinson, R.; Lloyd, A. C. *J. Phys. Chem. Ref. Data* **1984**, *13*, 315.

(2) Perner, D.; Platt, U.; Trainer, M.; Hubler, G.; Drummond, J.; Junkermann, W.; Rudolph, J.; Schubert, B.; Volz, A.; Elhalt, D. H. *J. Atmos. Chem.* **1987**, *5*, 185.

(3) Brider, W. C. *Combustion Chemistry*; Springer-Verlag: New York, 1984.

(4) Wang, B.; Hou, H.; Gu, Y. *J. Phys. Chem. A* **1999**, *103*, 8021.

(5) Zhou, Z.; Cheng, X.; Zhou, X.; Fu, H. *Chem Phys. Lett.* **2002**, *353*, 281.

(6) March, J. *Advanced Organic Chemistry*: *Reactions, Mechanisms, and Structure*, 4th ed.: John Wiley & Sons: New York, 1992.

(7) Herk, L.; Feld, M.; Szwarc, M. *J. Am. Chem. Soc.* **1961**, *83*, 2998.

(8) Skell, P. S.; May, D. D. *J. Am. Chem. Soc.* **1983**, *105*, 3999.

(9) Braun, W.; Rajbenbach, L.; Eirich, F. R. *J. Phys. Chem.* **1962**, *66*, 1591.

(10) Kieninger, M.; Ventura, O. N.; Suhai, S. *Int. J. Quantum Chem.* **1998**, *70*, 253.

(11) Rauk, A.; Yu, D.; Armstrong, D. A. *J. Am. Chem. Soc.* **1994**, *116*, 8222.

(12) Yu, D.; Rauk, A.; Armstrong, D. A. *J. Chem. Soc., Perkin Trans.* **1994**, *2*, 2207.

(13) Sicilia, E.; Di Maio, F. P.; Russo, N. *J. Phys. Chem.* **1993**, *97*, 528.

(14) Peyerimhoff, S. D.; Skell, P. S.; May, D. D.; Bunker, R. J. *J. Am. Chem. Soc.* **1982**, *104*, 4515.

(15) Feller, D.; Huyser, E. S.; Borden, W. T.; Davidson, E. R. *J. Am. Chem. Soc.* **1983**, *105*, 1459.

(16) Neumark, D. M. *Acc. Chem. Res.* **1993**, *26*, 33.

(17) Wang, L. S.; Ding, C. F.; Wang. X. B.; Nicholas, J. B. *Phys. Rev. Lett.* **1998**, *81*, 2667.

(18) Lu, Z.; Continetti, R. E. *J. Phys. Chem. A* **2004**, *108*, 9962.

(19) Kim, E. H.; Bradforth, S. E.; Arnold, D. W.; Metz, R. B.; Neumark, D. M. *J. Chem. Phys.* **1995**, *103*, 7801.

(20) Clemente, T. G.; Continetti, R. E. *J. Chem. Phys.* **2001**, *115*, 5345.

(21) Rientra-Kiracofe, J. C.; Tschumper, G. S.; Schaefer, H. F., III; Nandi, S.; Ellison, G. B. *Chem. Rev.* **2002**, *102*, 231.

(22) Yamdagni, R.; Kebarle, P. *Ber. Bunsen-Ges. Phys. Chem.* **1974**, *78*, 181.

(23) Tsuda, S.; Hamill, W. H. Ionization Efficiency Measurements by the Retarding Potential Difference Method. In *Advances in Mass Spectrometry*; Mead, W. L., Ed.; The Institute of Petroleum: London, UK, 1966; Vol. III, p 249.

(24) Muftakhov, M. V.; Vasil'ev, Y. V.; Mazunov, V. A. *Rapid Commun. Mass Spectrom.* **1999**, *13*, 1104.

(25) Wentworth, W. E.; Chen, E.; Steelhammer, J. C. *J. Phys. Chem.* **1968**, *72*, 2671.

(26) Wenthold, P. G.; Hrovat D. A.; Borden, W. T.; Lineberger W. C. *Science* **1996**, *272*, 1456.

(27) http://webbook.nist.gov

(28) Wang, X. B.; Woo, H. K.; Wang, L. S. *J. Chem. Phys.* **2005**, *123*, 051106-1-4.

(29) Wang, X. B.; Woo, H. K.; Kiran, B.; Wang, L. S. *Angew. Chem., Int. Ed.* **2005**, *44*, 2−5.

(30) Wang, L. S.; Ding, C. F.; Wang, X. B.; Barlow, S. E. *Rev. Sci. Instrum.* **1999**, *70*, 1957.

(31) Gilles, M. K.; Polak, M. L.; Lineberger, W. C. *J. Chem. Phys.* **1992**, *96*, 8012.

(32) Frisch, M. J.; Trucks, G. W.; Schlegel, H. B.; Scuseria, G. E.; Robb, M. A.; Cheeseman, J. R.; Montgomery, J. A., Jr.; Vreven, T.; Kudin, K. N.; Burant, J. C.; Millam, J. M.; Iyengar, S. S.; Tomasi, J.; Barone, V.; Mennucci, B.; Cossi, M.; Scalmani, G.; Rega, N.; Petersson, G. A.; Nakatsuji, H.; Hada, M.; Ehara, M.; Toyota, K.; Fukuda, R.; Hasegawa, J.; Ishida, M.; Nakajima, T.; Honda, Y.; Kitao, O.; Nakai, H.; Klene, M.; Li, X.; Knox, J. E.; Hratchian, H. P.; Cross, J. B.; Bakken, V.; Adamo, C.; Jaramillo, J.; Gomperts, R.; Stratmann, R. E.; Yazyev, O.; Austin, A. J.; Cammi, R.; Pomelli, C.; Ochterski, J. W.; Ayala, P. Y.; Morokuma, K.; Voth, G. A.; Salvador, P.; Dannenberg, J. J.; Zakrzewski, V. G.; Dapprich, S.; Daniels, A. D.; Strain, M. C.; Farkas, O.; Malick, D. K.; Rabuck, A. D.; Raghavachari, K.; Foresman, J. B.; Ortiz, J. V.; Cui, Q.; Baboul, A. G.; Clifford, S.; Cioslowski, J.; Stefanov, B. B.; Liu, G.; Liashenko, A.; Piskorz, P.; Komaromi, I.; Martin, R. L.; Fox, D. J.; Keith, T.; Al-Laham, M. A.; Peng, C. Y.; Nanayakkara, A.; Challacombe, M.; Gill, P. M. W.; Johnson, B.; Chen, W.; Wong, M. W.; Gonzalez, C.; Pople, J. A. *Gaussian 03*, Revision C.02; Gaussian, Inc.: Wallingford, CT, 2004.

(33) Bach, R. D.; Ayala, P. Y.; Schlegel, H. B. *J. Am. Chem. Soc.* **1996**, *118*, 12758.

(34) Woo, H. K.; Wang, X. B.; Kiran, B.; Wang, L. S. *J. Phys. Chem. A* **2005**, *109*, 11395.

(35) Lau, K. C. Private communication.